Zentrum für Technomathematik

Fachbereich 3 – Mathematik und Informatik

Numerical simulation of a silicon floating zone with a free capillary surface

Eberhard Bänsch **Burkhard Höhn**

Report 98–08

Berichte aus der Technomathematik

Report 98–08 **Dezember 1998**

Numerical simulation of a silicon floating zone with a free capillary surface

Eberhard Bänsch[1] and Burkhard Höhn[2]

[1] Zentrum für Technomathematik, FB 3, Universität Bremen, Postfach 330440, D-28334 Bremen, Germany
[2] Institut für Angewandte Mathematik, Universität Freiburg, Hermann–Herder Str. 10, D-79104 Freiburg, Germany

Abstract. In this article we present numerical results concerning the simulation of semiconductor melts with free capillary surfaces , particularly silicon crystal growth by the floating zone method. Considering the solid/liquid interface as fixed such a simulation requires the computation of the moving capillary surface of the melting zone. The mathematical model is a coupled system which consists of a heat equation and the Navier–Stokes equations in the melt with a Marangoni boundary condition. We describe an efficient numerical method for solving this problem and give some results for different physical parameters.

1 Introduction

Fluctuations of the electrical resistivity due to inhomogeneous dopant distribution are still a serious problem for the industrial processing of doped semiconductor crystals. In the case of silicon floating–zone growth, the main source of these inhomogeneities are time–dependent flows in the liquid phase during the growth process. Hence, for optimizing the growth process, it is of great importance to study the influence of thermocapillary and buoyancy convection on macro– and microsegregation, see [4–8]. A very practical experimental setup for these investigations is the floating–zone growth in a mono ellipsoid mirror furnace.

For instance, such a configuration has been successfully used at the Institute for Crystallography, University of Freiburg, for performing silicon floating–zone experiments on earth and also under microgravity, see e.g. [5]. A halogen lamp, positioned in the upper geometrical focus of the ellipsoid, served as a heat source. Fused quartz ampoules containing the starting material were placed in the lower geometrical focus. The parameters of the liquid zone were as follows: $8mm$ zone height and $12mm$ zone diameter. Figure 1 shows both, the surface of the silicon melt and an etched axial cut of the zone showing the solid–liquid interface.

Due to the opaqueness of semiconductor melts, experimental fluid flow observation is extremely difficult and expensive in general. Therefore the numerical simulation of the growth process is an important tool in understanding and predicting the behavior of the system, see e.g. [6].

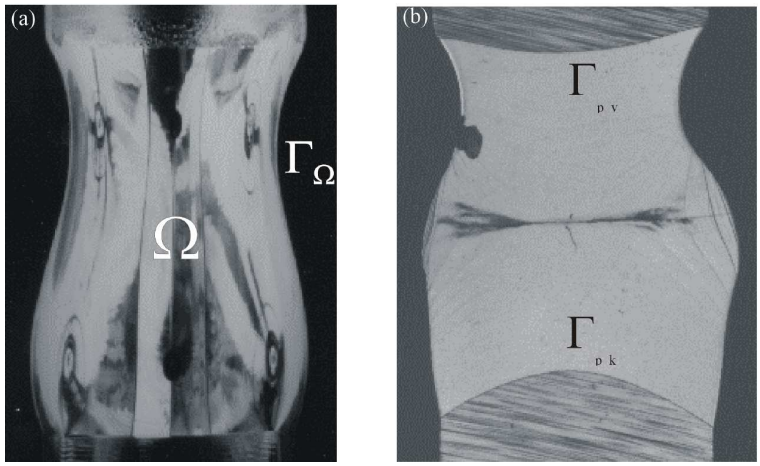

Fig. 1. Silicon floating zone: (a) Surface of the silicon melt, (b) Etched axial cut of the zone showing the solid–liquid interface

2 Mathematical model

Figure 2 gives a schematic diagram of a floating–zone configuration.

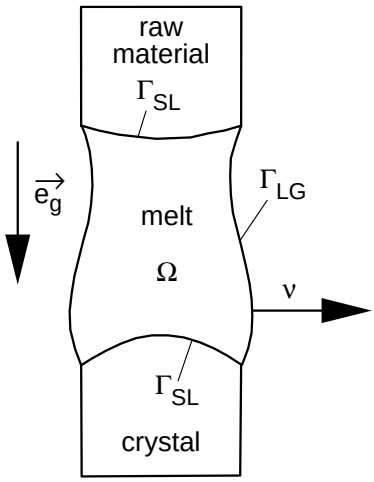

Fig. 2. Geometry of a floating zone

The heat and mass transfer in the liquid zone is governed by the following system of partial differential equations (in dimensionless form):

- Navier–Stokes equations:

$$\begin{aligned} \partial_t u + (u \cdot \nabla)u - \frac{1}{Re}\Delta u + \nabla p &= -\frac{Ra}{Re^2 Pr} T \boldsymbol{e}_g && \text{in } \Omega(t) \\ \nabla \cdot u &= 0 && \text{in } \Omega(t) \end{aligned} \tag{1}$$

- Energy equation:

$$\partial_t T \; + \; u \cdot \nabla T - \frac{1}{Re\, Pr}\Delta T \; = \; 0 \quad \text{in } \Omega(t) \tag{2}$$

Here $u(t,\cdot) : \Omega(t) \to I\!R^d$, $p(t,\cdot) : \Omega(t) \to I\!R$ and $T(t,\cdot) : \Omega(t) \to I\!R$ denote the flow velocity, the pressure and the temperature, respectively.
The interfaces Γ_{SL} and Γ_{GL} are free boundaries, the first one being subject to a Stefan condition, the latter one determined by a balance of capillary forces versus normal stresses of the flow. We simplify the problem by focusing on the free boundary conditions on Γ_{LG} and prescribing a given solid–liquid interface Γ_{SL} where we impose a homogeneous Dirichlet boundary condition for u and T ($T = 0$ the dimensionless melting temperature):

$$u = 0 \quad \text{on } \Gamma_{SL}\,, \tag{3}$$

$$T = 0 \quad \text{on } \Gamma_{SL}\,. \tag{4}$$

Note that prescribing Γ_{SL} implies that also the $d-2$ dimensional *tripleline* (or *triplepoint* for $d = 2$) $\Gamma_{LG} \cap \Gamma_{SL}$ is prescribed and fixed. On the free liquid–gas interface the temperature is prescribed by a given parabolic profile:

$$T = T_D \quad \text{on } \Gamma_{LG}\,. \tag{5}$$

For the velocity and the motion of the free surface the following conditions hold on Γ_{LG}:

$$u \cdot n = V_\Gamma \quad \text{(slip boundary condition)} \tag{6}$$

$$n \cdot \sigma\tau = -\frac{Ma}{Re^2 Pr}\nabla T \cdot \tau \quad \text{(Marangoni condition)} \tag{7}$$

$$n \cdot \sigma n = \frac{1}{ReCa}\kappa + \frac{Bo}{ReCa}\,\mathrm{id}_\Gamma \cdot \boldsymbol{e}_g \quad \text{(normal stress condition)} \tag{8}$$

with $\sigma := \left(\frac{1}{Re}D(u)_{ij} - p\,\delta_{ij}\right)_{i,j=1}^{d}$ the stress tensor, $D(u) := \left(\partial_{x_i}u_j + \partial_{x_j}u_i\right)_{i,j=1}^{d}$ the deformation tensor, κ the sum of the principal curvatures, the unit outer normal vector n, an arbitrary tangential vector τ and the normal velocity V_Γ of the free boundary Γ_{LG}.
The system has to be closed by initial conditions for u, T and Ω. Note that in the continuous case we have conservation of volume since the velocity u is divergence free.
The dimensionless numbers occurring in the above equations are the Reynolds number $Re = \dfrac{U\,L}{\nu}$, the Prandtl number $Pr = \dfrac{\nu}{k}$, the Rayleigh number

$Ra = \frac{g\beta\delta T L^3}{k\nu}$, the Marangoni number $Ma = -\frac{(\partial\gamma/\partial T)\delta T L}{k\rho\nu}$, the capillary number $Ca = \frac{\nu\rho U}{\gamma}$ and the Bond number $Bo = \frac{\rho g L^2}{\gamma}$, with a characteristic velocity U, a characteristic length L, a characteristic temperature difference δT, the density ρ, the surface tension γ, the thermal coefficient $\partial\gamma/\partial T$ of surface tension, the thermal diffusivity k, the kinematic viscosity ν and the gravitational acceleration g.
Stationary, two dimensional numerical methods for the above free boundary problem were studied for instance in [4]. However, even if all data are rotationally symmetric or two dimensional according to the physical setup, the solution may be expected to be 3D and also time–dependent due to symmetry breaking. Thus, it is necessary to define a numerical scheme for the time–dependent case and which works also in 3 space dimensions.

3 Numerical approximation

Discretizing equations (1)–(8), the free boundary conditions (6)–(8) cause several problems, in particular the treatment of the curvature terms and in finding a stable and efficient time discretization.
To resolve these problems we use a variational formulation, where the free boundary conditions are transformed to a boundary integral part of the bilinear forms, see [2] for details. To this end we write the momentum part of the Stokes equations (analogously for the Navier–Stokes equations) in the strong form, multiply by a solenoidal test function φ and integrate by parts. We get

$$\int_\Omega \{-\frac{1}{Re}\Delta u + \nabla p\} \cdot \varphi = \frac{1}{2Re}\int_\Omega D(u) : D(\varphi) - \int_\Omega p\nabla\cdot\varphi - \int_{\Gamma_{LG}} n\cdot\sigma\varphi.$$

Taking into account the boundary conditions (7,8) yields

$$\int_{\Gamma_{LG}} n\cdot\sigma\varphi = -\frac{Ma}{Re^2 Pr}\sum_{i=1}^{d-1}\int_{\Gamma_{LG}} \nabla T\cdot\tau_i\,\varphi\cdot\tau_i + \frac{Bo}{ReCa}\int_{\Gamma_{LG}} \mathrm{id}_{\Gamma_{LG}}\cdot\boldsymbol{e}_g\varphi\cdot n + \frac{1}{ReCa}\int_{\Gamma_{LG}} \kappa\, n\cdot\varphi. \tag{9}$$

Now we make use of the identity

$$\underline{\Delta} id_{\Gamma_{LG}} = \kappa\, n, \tag{10}$$

where $\underline{\Delta}$ denotes the Laplace Beltrami operator on Γ_{LG}. Recalling that $\underline{\Delta} = \underline{\nabla}\cdot\underline{\nabla}$ with $\underline{\nabla}$ the tangential derivatives, the last term in (9) can be written

as

$$\int_{\Gamma_{LG}} \kappa\, n \cdot \varphi = \int_{\Gamma_{LG}} \underline{\Delta}\mathrm{id}_{\Gamma_{LG}} \cdot \varphi = -\int_{\Gamma_{LG}} \underline{\nabla}\mathrm{id}_{\Gamma_{LG}} \cdot \underline{\nabla}\varphi. \tag{11}$$

Summarizing we get

$$\begin{aligned}\int_{\Omega} \{-\frac{1}{Re}\Delta u + \nabla p\} \cdot \varphi = \frac{1}{2Re}\int_{\Omega} D(u) : D(\varphi) - \int_{\Omega} p\,\nabla \cdot \varphi \\ + \frac{1}{ReCa}\int_{\Gamma_{LG}} \underline{\nabla}\mathrm{id}_{\Gamma_{LG}} \cdot \underline{\nabla}\varphi \\ + \frac{Ma}{Re^2 Pr}\sum_{i=1}^{d-1}\int_{\Gamma_{LG}} \nabla T \cdot \tau_i \varphi \cdot \tau_i \\ - \frac{Bo}{ReCa}\int_{\Gamma_{LG}} \mathrm{id}_{\Gamma_{LG}} \cdot \boldsymbol{e}_g \varphi \cdot n\end{aligned} \tag{12}$$

Time discretization To discretize in time a semi–implicit coupling of the unknowns for temperature T, geometry Ω and the flow variables u, p is used. More precisely, giving the values at the discrete time instant t_{k-1} we compute

Step 1: T^k by solving (2) on Ω^{k-1} with u^{k-1}

Step 2: u^k, p^k by solving (1) with boundary conditions (7,8) on Ω^{k-1} and using T^k on the right hand side

Step 3: Γ_{LG}^k by $\Gamma_{LG}^k := \Gamma_{LG}^{k-1} + (t_k - t_{k-1})\, u^k \cdot n\, n$

In **Step 2** the boundary conditions (7,8) are incorporated into the variational formulation according to (12). The curvature terms are treated in a semi–implicit way:

$$\int_{\Gamma_{LG}^{k-1}} \underline{\nabla}\mathrm{id}_{\Gamma_{LG}^k} \cdot \underline{\nabla}\varphi = \int_{\Gamma_{LG}^{k-1}} \underline{\nabla}\mathrm{id}_{\Gamma_{LG}^{k-1}} \cdot \underline{\nabla}\varphi + (t_k - t_{k-1})\int_{\Gamma_{LG}^{k-1}} \underline{\nabla}u^k \cdot \underline{\nabla}\varphi,$$

thus decoupling the flow computation from the determination of the geometry. This leads to a stable and efficient treatment of the free boundary conditions, see [2].
The computation of u^k, p^k is based on the fractional step θ–scheme in a variant as an operator splitting, which decouples two major numerical difficulties, the solenoidal condition and the nonlinearity, see [1,3].

Spatial discretization To discretize in space piecewise quadratic, globally continuous elements for u and T and piecewise linear, globally continuous elements for p are used on a tetrahedral grid.

4 Numerical results

The following two examples show the influence of the hydrostatic pressure on the shape of a floating zone with aspect ratio $h/d = 1.5$. Here $g_E = 9.81m\,s^{-2}$ denotes the gravitational acceleration on earth.

Example 1 First we consider a 2D–floating zone with buoyancy convection and no thermocapillary convection, i.e. $Ma = 0$. The dimensionless parameters are chosen as follows: $Re = 500$, $Pr = 0.02$, $Ca = 0.0016$, $Ra = 400 * |g|$, $Bo = 0.18 * |g|$ with $g \in \{0.5 * g_E, 2.0 * g_E, 3.5 * g_E\}$. Figures 3 – 5 show both the velocity field together with the temperature distribution in the melt and the corresponding triangulation of the domain Ω.

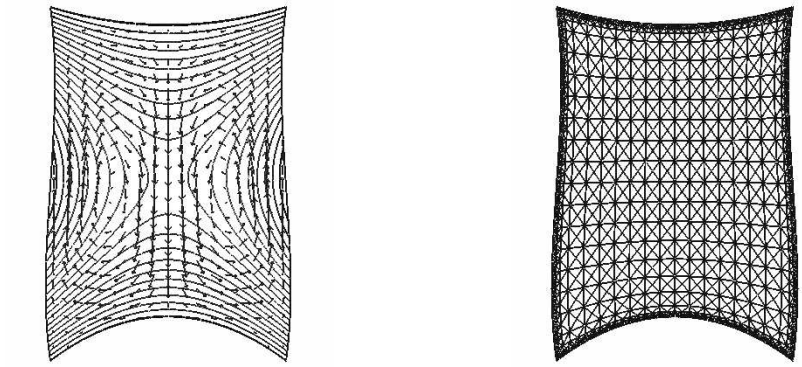

Fig. 3. Velocity field, temperature distribution and triangulation for $g = 0.5 * g_E$

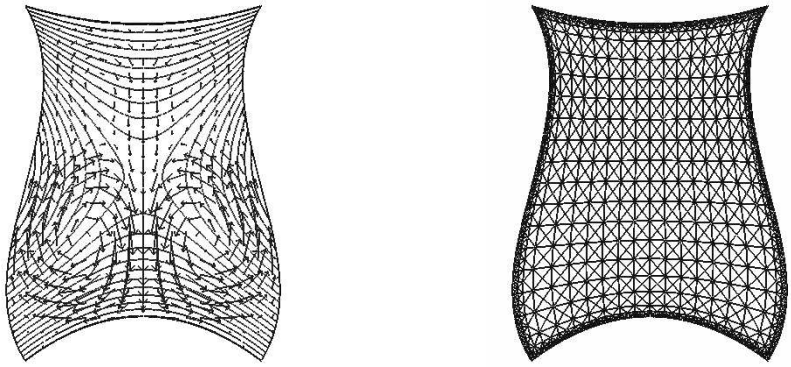

Fig. 4. Velocity field, temperature distribution and triangulation for $g = 2.0 * g_E$

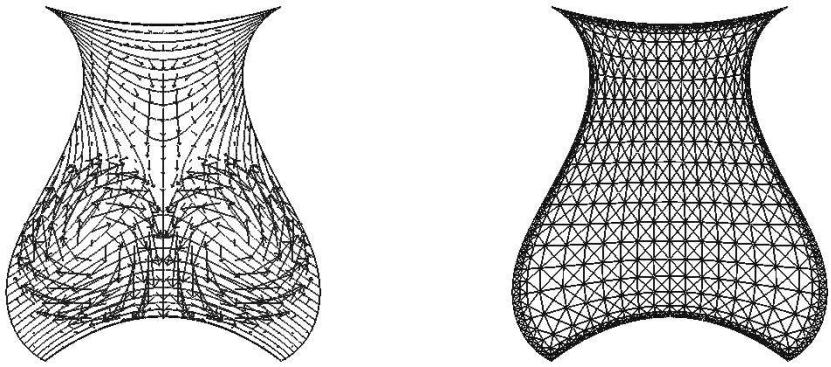

Fig. 5. Velocity field, temperature distribution and triangulation for $g = 3.5 * g_E$

Example 2 Now let us consider a 3D–floating zone with Marangoni convection and no buoyancy convection, i.e. $Ra = 0$. The other dimensionless parameters are: $Re = 50$, $Pr = 2$, $Ma = 150$, $Ca = 0.016$, $Bo = 0.18 * |g|$ with $g \in \{0, 1.0 * g_E, 2.0 * g_E\}$. Figures 6 – 8 show both the velocity field together with the temperature distribution in the melt and the corresponding triangulation of the domain Ω.

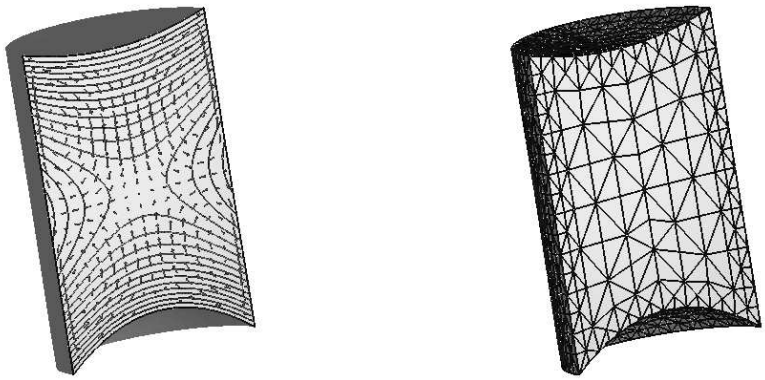

Fig. 6. Velocity field, temperature distribution and triangulation for $g = 0$

References

1. E. BÄNSCH, *Simulation of instationary, incompressible flows*, Acta Math. Univ. Comenianae LXVII, no. 1, 101–114 (1998)
2. E. BÄNSCH, *Numerical methods for the instationary Navier–Stokes equations with a free capillary surface*, Habilitation thesis, Univ. Freiburg (1998).

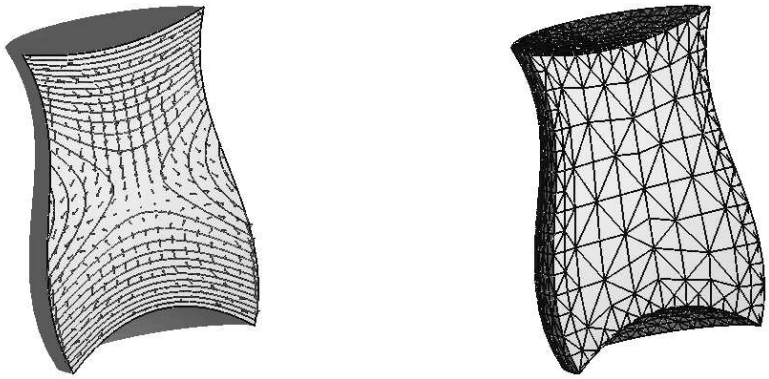

Fig. 7. Velocity field, temperature distribution and triangulation for $g = 1.0 * g_E$

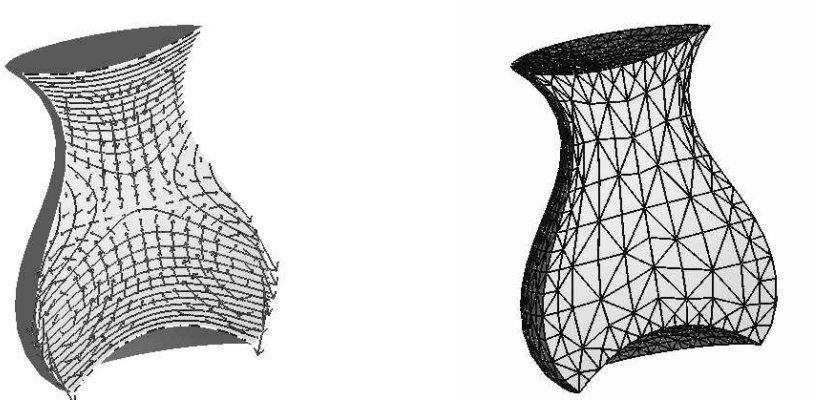

Fig. 8. Velocity field, temperature distribution and triangulation for $g = 2.0 * g_E$

3. M. O. Bristeau, R. Glowinski and J. Periaux, *Numerical methods for the Navier–Stokes equations. Application to the simulation of compressible and incompressible flows*, Computer Physics Report, 6 (1987), pp. 73–188.
4. C. Cuvelier and J. M. Driessen, *Thermocapillary free boundaries in crystal growth*, J. Fluid mech., vol. 169 (1986), pp. 1–26.
5. P. Dold and A. Cröll and K. W. Benz, *Floating–zone growth of silicon in magnetic fields, Part I: Weak static axial fields*, J. Crystal Growth, 183 (1998), pp. 545–553.
6. T. Kaiser and K. W. Benz, *Floating–zone growth of silicon in magnetic fields, Part III: Numerical simulation*, J. Crystal Growth, 191 (1998), pp. 365–376.
7. G. Müller and A. Ostrogorsky, *Convection in Melt Growth*, in Handbook of Crystal Growth 2B, D. T. J. Hurle, eds., Elsevier Science Publishers, North-Holland, 1994, pp. 709-819.
8. D. Schwabe, *Surface–Tension–Driven Flow in Crystal Growth Melts*, in Crystal Growth, Properties and Applications 11, Springer, Berlin, 1988.

Berichte aus der Technomathematik ISSN 1435-7968

http://www.math.uni-bremen.de/zetem/berichte.html

— Vertrieb durch den Autor —

Reports **Stand: 16. November 1998**

98–01. Peter Benner, Heike Faßbender:
An Implicitly Restarted Symplectic Lanczos Method for the Symplectic Eigenvalue Problem, Juli 1998.

98–02. Heike Faßbender:
Sliding Window Schemes for Discrete Least-Squares Approximation by Trigonometric Polynomials, Juli 1998.

98–03. Peter Benner, Maribel Castillo, Enrique S. Quintana-Ortí:
Parallel Partial Stabilizing Algorithms for Large Linear Control Systems, Juli 1998.

98–04. Peter Benner:
Computational Methods for Linear–Quadratic Optimization, August 1998.

98–05. Peter Benner, Ralph Byers, Enrique S. Quintana-Ortí, Gregorio Quintana-Ortí:
Solving Algebraic Riccati Equations on Parallel Computers Using Newton's Method with Exact Line Search, August 1998.

98–06. Lars Grüne, Fabian Wirth:
On the rate of convergence of infinite horizon discounted optimal value functions, November 1998.

98–07. Peter Benner, Volker Mehrmann, Hongguo Xu:
A Note on the Numerical Solution of Complex Hamiltonian and Skew-Hamiltonian Eigenvalue Problems, November 1998.